MEASUREMENTS OF CARBON FLUXES DURING LOW PRESSURE CARBURIZING

Philippe JACQUET[1] and Daniel R. ROUSSE[2✉]

[1] LABOMAP, Ecole Nationale Supérieure d'Arts et Métiers,
71 250 Cluny, France
Tel : 33 03 85 59 53 28 ; Fax : 33 03 85 59 53 70
jacquet@cluny.ensam.fr

[2] Département de génie mécanique, Université Laval,
Sainte-Foy (Québec), Canada G1K 7P4
Tel : 001 418 656 2131 (3345) ; Fax : 001 418 656 7415
Daniel.Rousse@gmc.ulaval.ca

✉ *Author to whom further correspondence should be addressed.*

ABSTRACT

This paper presents the qualitative assessment of a novel device developed for the regulation of carburizing processes in industrial vacuum furnaces. The proposed device involves a U-shaped thin wall iron tube: the outside surface of the tube is exposed to the carburizing atmosphere simultaneously with the workload, while the decarburizing gas mixture (here H_2 + H_2O) is circulated inside the tube. The outflow of decarburizing mixture is then continuously analyzed and eventually permits to determine the carbon potential and the transfer coefficient at the interface between the carburizing atmosphere and the workloads. To assess the principle, the probe has been used to compare the carburizing power of different gases (propane, methane, ethylene, and acetylene) for a specific set of parameters. The results reported here, compared with microhardness and micrographies of the samples, indicate that the probe can indeed be used to carry out this task.

Key words : **carburizing, U-shaped thin wall sensor, control**

NOMENCLATURE

C	Carbon concentration, %
D	Mass diffusion coefficient, cm^2/s
K	Mass transfer coefficient, cm/s
L	Sensor wall thickness, μm
Q	Activation energy, J/mol
P	Pressure, bar, mbar
R	Constant, 8.314 J/mol K
S	Rate of generation (dissolution) of carbon, %/s
t	Time, s, min, h
T	Temperature, K
V	Volumetric flow rate, mL/min
x	Spatial position within the wall of the tubular probe, m

Indices and superscripts

0	Reference condition
a	Related to the gas activation energy
C	Carburizing
d	Related to the solid activation energy, diffusion
dew	Dew point
D	Decarburizing
G	In the decarburizing gas
i	Gas-solid interface
P	Carbon potential
s	Saturation
t	Transition in the chamber

1. INTRODUCTION

The main advantages of low pressure carburizing treatments compared to the atmospheric gaseous processes are now well known: faster kinetics and oxygen free carburizing atmospheres resulting in carburized layers that involve no internal oxidation [1]. For two decades, several low pressure carburizing processes have been developed: plasma carburizing with methane [2]; "boost-diffusion" carburizing with propane [3]; carburizing with various ethylene flows [4]; vacuum carburizing with acetylene [5]; the i-Vacarb® process [6]. Each of these processes try to eliminate the problem of soot formation inside the furnace. When atmospheres are too rich in carbon, either some soot can form a deposit on the steel's surface and stop further carbon diffusion or some undesirable carbides can appear.

Hence, regulation is needed. However, to the best knowledge of the authors, no regulation process has been made available in the context of low pressure carburizing treatments. To date, none of the existing devices that monitor the carbon potential at atmospheric pressure [7,8] can be used under low-pressure conditions. This is usually due to the absence of thermodynamic equilibrium [9-10]. As a result, the low pressure carburizing processes is solely modeled by computer [11-15]. Hence, although low pressure carburizing can be more efficient than atmospheric carburizing, the lack of appropriate regulation devices seems to stand in the way of its development.

In this context, this paper presents a novel sensor designed, constructed and tested to bridge the gap between this need for regulation in low-pressure atmospheres and the increased performance of carburizing in such conditions. The probe's principle has first been tested in a small experimental furnace [16] and has been presented in a previous paper [17]. The aim of the research is to determine whether or not the device could be used to predict carburizing rates and carbon content in workloads. This research effort mainly involves a qualitative assessment of the probe which is used here inside an industrial low pressure furnace.

In this paper, the carburizing process is first recalled, then the experimental environment with the new U-shaped tubular sensor and the vacuum furnace are presented. The following section deals with the experimental parameters used and the last one offers the metallurgical results and the probe's recording data.

2. CARBURIZING PROCESS

2.1 Physics of carburizing

The physics of carbon diffusion as applied to the proposed U-shaped sensor is shown in Figure 1. In this figure, the outer surface of a thin iron tube is exposed to a carburizing furnace atmosphere while a controlled decarburizing environment flows on the inner side of this thin U-shaped sensor. In the experiments, several carburizing gases have been used inside the furnace : methane CH4, acetylene C2H2, ethylene C2H4, and propane C3H8. The principle of control is based on the fact that when steady state is reached in the wall of the circular-shaped tubular sensor, the measured mass flux of carbon on the inside (decarburizing) is related to the inflow of carbon into the parts during the carburizing treatment. Hence, as a probe can be inserted directly into the furnace, it provides an *in-situ* control facility. It can be noted that if the saturation concentration of carbon, C_s, is reached within the wall of the tube, normally at the carburizing surface first, precipitation of carbides (Fe_3C) will occur. On the other hand, if the tube is not quenched, when the carbon concentration decreases below C_s, anywhere within the wall thickness, the carbides will be dissolved.

2.2 Mathematical description of carbon diffusion

The basis for modeling single phase carburizing is the following mass balance equation which states that the total carbon in a differential volume changes in time according to the divergence of the carbon flux plus a volumetric source term of carbon that accounts for carbide precipitation or dissolution:

$$\frac{\partial C(x,t)}{\partial t} = \frac{\partial}{\partial x}\left(D(x,t)\frac{\partial C(x,t)}{\partial x}\right) + S_C(x,t)\,;\ 0 \le x \le L;\ t>0 \tag{1}$$

in which x is the distance from the carburizing surface, L is the wall thickness, C is the carbon concentration, D is the mass diffusion coefficient, and S_C is the volumetric source of carbon (it is negative in the case of carbides precipitation and positive when carbides are dissolved in the matrix). The equation is strictly valid in the Cartesian coordinate system as well as for cylindrical or spherical shells for which the wall thickness, L, is much smaller than the radii. The boundary and initial conditions are then:

$$K_C(t)(C_P - C(x,t)) = -D(x,t)\frac{\partial C(x,t)}{\partial x};\quad x=0;\quad t>0 \tag{2}$$

$$K_D(t)(C(x,t) - C_G) = -D(x,t)\frac{\partial C(x,t)}{\partial x};\quad x=L;\quad t>0 \tag{3}$$

$$C(x,0) = C_i;\quad 0 \le x \le L;\quad t=0 \tag{4}$$

where K_C is the mass transfer coefficient on the carburizing side, K_D is the mass transfer coefficient on the decarburizing side, C_P is the carbon potential of the carburizing atmosphere, C_G is the carbon potential of the decarburizing gas, C_G =0, and C_i is the initial concentration of carbon in the material. C_i could be a function of x but for the situations involved here, the initial carbon concentration was considered uniform and equal to zero throughout the wall.

The expressions for D and K have been correlated by several authors for different steels. Ghiglione [18] proposes a review that involves 13 different expressions for D and 9 for K. Here, the following forms are assumed [10]:

$$D(t) = D_0(C)\exp\left(-\frac{Q_d}{RT}\right) \tag{5}$$

$$K_D(t) = K_{D,0}\exp\left(-\frac{Q_a}{RT}\right) \tag{6}<$$

in which Q_d is the activation energy of carbon diffusion in austenite, Q_a is the activation energy of the carburizing atmosphere, R=8.314 J/mol K, and T is the temperature in Kelvin. This model forms the basis for all subsequent numerical analysis as well as for the variables to be measured with the experimental apparatus. Variables to be provided to validate the numerical model.

2.3 Low pressure carburizing settings

For all the processes mentioned in section 1, the first step, which consists in a pumping period, is common; the heating phase then occurs under a vacuum or a nitrogen (oxygen free) atmosphere, that allows to eradicate the risk of internal intergranular oxidation. The main differences among the different processes appear during the carburizing period and relate to: the nature of the carburizing gas, the fluid velocities or mass flow rates, the operating pressure, the type (continuous or discontinuous) of injection, the type of mixture (single or multi phase), the presence of plasma, etc...

In this work, the carburizing power of the most commonly used gases have been compared; all the experiments have been performed under the same conditions of pressure, flow, and period. All experiments were carried out with pure gases.

3. EXPERIMENTAL FURNACE

3.1 Principle for monitoring

The physics of carbon diffusion as applied to the proposed device is simple: one side of a thin iron foil is exposed to a carburizing furnace atmosphere while the other side of this thin foil is exposed to a controlled decarburizing environment. Carbon atoms react at the carburized surface of the device and diffuse across its thickness, L. The flux of carbon at the decarburizing surface can then be measured. The principle of control is based on the fact that when steady state is reached in the iron foil, the measured mass flux of carbon on the decarburizing side of the foil is related to the inflow of carbon into the parts (workload) during the carburizing treatment. Hence, as a probe can be inserted directly into the furnace, it provides an *in-situ* control facility. In [16,17], the authors demonstrated that the principle can indeed be applied to predict carbon diffusion across workloads.

3.2 Sensor

The sensor was configured as a thin-wall U-shaped iron tube (thickness, L=100µm) and located inside the furnace. The outside surface of the tube is exposed to the carburizing atmosphere simultaneously with the workload, while the decarburizing gas mixture (here H_2 + H_2O) is circulated inside the tube. Once carbon atoms emerge from the inner surface of the tube, the decarburizing reactions produce carbon monoxide, CO, and methane, CH_4. The outflow of decarburizing gas was initially analyzed by a catharometer [16, 17], for more precision and convenience it is now analyzed by use of an hygrometer.

Figure 1 shows a schematic and a picture of the proposed device. Such a probe allows an *in situ* measurement of the carbon potential and the transfer coefficient at the interface between the atmosphere and the steel.

3.3 Furnace specifications

The BMI B 83 TiC vacuum furnace is a horizontal double-wall water cooled facility. It is entirely controlled and monitored with a custom software allowing to program treatment cycles, to recover data, etc. This furnace is a prototype that was specially designed and built for ENSAM. It allows for several types of low pressure heat treatments (carburizing, carbonitriding), brazing as well as plasma treatments (ionic nitriding, ionic carburizing). Figure 2 presents a schematic of the transversal section of the furnace.

The furnace involves a hydraulic frontal loading door that operates in conjunction with the casing door, longitudinal slots allows for the cooling flow, and cooper cooling coils monitored for security purposes. The furnace allows radiant and convective heating and enables homogeneous and rapid cooling of the load by forced convection of nitrogen ($1<P<5$ bar) that is circulated through an efficient exchanger. The cooling system is included inside an airtight casing. The pressure, the velocity, and the direction of the nitrogen flow can be specified.

Figure 2 shows the centrifugal turbine driven by a sealed and cooled motor located axially, the casing with the workload support, the 40 m^2 finned-tubes heat exchanger, and the patented cooling turbine [16, 17].

The chamber is $450 \times 450 \times 450$ mm and can allow for a load of approximately 100 kg. The maximum operating temperature is 1200°C, the minimum vacuum pressure is about 10^{-2} mbar, and the working pressure during heat treatments lies between 1 and 10 mbar. Up to four different gases can be mixed together.

The radiation heating is obtained by a cage-shaped graphite resistance which surrounds the load for an optimal heat transfer. For a more efficient heat transfer at low temperatures, a forced convection heating system is used. The atmosphere is forced by a carbon/carbon composite fan.

4. COMMON EXPERIMENTAL PARAMETERS

4.1 Carburizing parameters

For each experiment presented in this paper, the carburizing cycle involved the following parameters: a pumping period to decrease the pressure to P=0.1 mbar (0.075 torr); a heating period to T_∞=980°C (1796°F); a carburizing period at 6 mbar (4.5 torr) with a 5 L/min flow of carburizing gas; a diffusion period, and finally a 5 bar (3750 torr) quenching period with nitrogen.

For each experiment, a thermocouple has been inserted inside a reference workload in order to control the temperature (which remained constant at 980°C during all the cycle (carburizing + diffusion)).

All samples used, for results presented herein, were made of *25 CrMo 4* steel. The chemical composition of this alloy has been determined by means of a spark spectrometer. The following results have been obtained: *C*: 0.24%, *Si*: 0.22%, *Mn*: 0.63%, *Ni*: 0.13%, *Cr*: 1.14%, and *Mo*: 0.19%. This material has been chosen for its high quenching ability as the 5 bar gas quenching is less efficient than oil quenching.

4.2 Decarburizing parameters

The decarburizing mixture (which flows inside the tubular sensor) involves hydrogen and water vapor, $H_2 + H_2O$. The pressure is P=1 bar (750 torr), the dew point is T_{dew}= 2°C, and the volumetric flow rate V=50mL/min. The moisture content in mixture is measured with a hygrometer over a range of –110 to 60°C (-166 to 140°F). The moisture probe consists of an aluminum oxide sensor located on a connector and covered by a protective stainless-steel shield. Before mixture with water vapor, the dew point of hydrogen is T_{dew} = -40°C.

At the inner face of the iron tube, the following reactions occur:

$$C + H_2O \rightarrow CO + H_2 \quad (7)$$

$$C + 2\,H_2 \rightarrow CH_4 \quad (8)$$

A dew point of 2°C for the decarburizing mixture has been chosen for the following reasons: the higher the dew point, the faster the decarburizing reaction [20]; the environment temperature should be at least 10°C higher than the dew point temperature, otherwise condensation could occur on the sensor or in sampling system; the dew point should not be too high to avoid oxidation of iron; some results [21] showed that for a dew point higher of about 7°C, the second reaction, eq.(8), can be neglected. As the experiments were carried out for a dew point temperature not very far away from 7°C (2°C), the second reaction, eq. (8), has been neglected in the following analysis.

Nevertheless, a mixture of nitrogen and water has also been tried out as the decarburizing gas, thus eliminating the possibility of methane production, eq. (8). This would have enable a precise quantitative analysis of the rate of carbon diffusion across the thin wall of the probe. However, the decarburizing mixture for which no hydrogen is involved leads to the combination of oxygen atoms with iron, thus permitting severe oxidation of the probe. It was found absolutely necessary to inject at least a tiny fraction of hydrogen in the decarburizing mixture.

5. RESULTS

5.1 Probe response

As qualitative results are desired and because eq.(8) is neglected in the analysis of the mass flow rates of carbon, results in Figure 3 and 4 are presented in terms of the dew point of the decarburizing mixture. As the dew point drops, more water molecules are converted into carbon monoxide and hydrogen. Hence, the dew point is an indicator of the carbon flux across the wall thickness of the tubular probe.

The decarburizing gas grabs carbon as it travels within the probe. Hence, the radial flux of carbon varies along the probe axis and the amount of carbon detected is an average of the mass flow rate of carbon across the wall thickness. Moreover, the kinetic of carburizing and particularly decarburizing is quite slow. Hence, there is a need for investigations concerning the appropriate manners to obtain mass flow rates of carbon through a workload based on the dew points measurements. Work is actually being done on this subject.

Figure 3 shows the experimental results obtained for a 90s carburizing period with propane. The carburizing followed by a 40min diffusion period. Forty seconds after the injection, a fast increase of the signal (a sharp decrease of the dew point) is recorded. The water content decrease indicates that the carbon that is crossing the wall combines with water (eq.(7)).

The 40s delay corresponds to the time required by carbon to cross through the wall of the probe (L=100µm). After 90s, the injection of the carburizing gas is stopped and a pumping period begins; the pressure drops inside the furnace. Nevertheless, the signal is still increasing which indicates that more and more carbon emerge from the inner surface of the tube, then this signal reaches a maximum ($T_{dew} \approx$ -20°C) which corresponds to the maximum carbon flux. This maximum is obtained approximately 10 min after the end of the carburizing period. Then, as there is no quenching, the signal is slowly decreasing down to the original value (T_{dew} = 2°C); the time required to extract all carbon is longer than that to reach the maximum flux which means that the kinetic of the decarburizing reaction is slower than that of carburizing.

The repeatability of the experiments was investigated prior to the publication of this paper and is discussed elsewhere [17]. For the same set of parameters, the probe curbs corresponds within about 1% [17].

Figure 4 shows results for four carburizing treatments of a given work load with different gases: methane (CH_4), acetylene (C_2H_2), ethylene (C_2H_4), and propane (C_3H_8). Both carburizing and decarburizing parameters are the same as described previously. For all four cases, the carburizing period is 10 min and the diffusion period, before the quenching, is 15min.

Figure 4 reveals that the signal provided by the probe is very low for methane. This indicates that methane (subject to with these conditions, P=6mbar, T=980°C) is a very poor carburizing atmosphere. Figure 5 and 6 confirm the information provided by the probe.

For the other three gases (acetylene, ethylene and propane), the shape of the signals is the same as that observed in Figure 3: it increases about forty seconds after the injection of the carburizing gas and the maximum carbon flux is obtained approximately 10min after the end of the carburizing period. After quenching, the signals suddenly drop back to the initial for the dew point: the quench stops carbon diffusion inside the tube and consequently the decarburizing reaction.

For acetylene and ethylene the signals are very close whereas for propane, the maximum carbon flux is slightly higher (T_{dew} = -21°C for C_3H_8, T_{dew} = -18°C for C_2H_2 and C_2H_4). This indicate that the carburizing power of propane should be somewhat higher than acetylene or ethylene. Theoretically, this is due to the fact that a propane molecule can leave three carbon atoms while an acetylene or ethylene molecule only two. However, the differences could also be due to the fact that a different path for injection has been used with propane. More investigations should be carried out to conclude on this topic. For high flow rates of carburizing gases, soot formation inside furnaces has been observed with propane, never with acetylene or ethylene [22].

Figure 4 shows deflections of the curves for C_2H_2, C_2H_4 and CH_4 at about t= 660s while there is no such deflection for C_3H_8. These “bumps” are due to the fact that when the carburizing ends with the first 3 gases, the heating is stopped while a vacuum pump (0,5 mbar) evacuates the gas. For C_3H_8 only, the injection of a nitrogen flow into the furnace that removes the carburizing atmosphere. As a result, there is no temperature drop in the furnace for C_3H_8 and the curve exhibits a smooth behavior.

5.2 Microhardness and micrographies

Microhardness measurements of the parts have been performed on a LECO AMH-100, a fully automated microhardness tester with programmable X-Y stage. For the tests reported here, it is configured with a Vickers diamond indenter. A stage pattern of 21 points has been defined: a 50µm-X and 100µm-Y space between the 11 first points, a 100µm-X space between the 5 following ones and a 200µm-X space between the 5 last ones. The pattern is followed by the stage and indentations are made on each position of the sample (with a 200g load). Once this is done, the pattern will be followed a second time for measuring the size of the indentations. From these measurements, calculations are made taking into consideration all the system's settings including calibrations.

Figure 5 shows the hardness as a function of the depth in the part after quenching. The figure clearly shows that the probe is adequate: methane is not efficient for carburizing in the experimental conditions used no hardness elevation is noticed on figure 5. The figure also shows that a carburizing depth (Hv ≥ 550) of 240µm is measured for each other three gases.

Micrographies have been obtained with a DP10 microscope digital camera system which is mounted on a VANOX-T Olympus microscope. The camera is connected to a PC for the storage of the pictures.

Figure 6 also confirm the preceding quantitative results, Figure 6a indicates that no carburized layer is observed for methane. Acetylene, ethylene and propane lead to similar results (Figs. 6a-6c) an approximately 200µm martensitic layer is formed. Moreover, the curves for C_2H_2 and C_2H_4 in Figure 4 are close to each other and Figure 6b and 6c show a more or less identical behavior after the quenching. Figure 6d also shows that more carbon has penetrated through the sample while carburizing with C_3H_8.

This is also predicted by the probe as curve for C_3H_8 in Figure 4 is higher than that for C_2H_2 and C_2H_4.

6. CONCLUSION

The aim of this paper is to demonstrate that a principle implemented in a laboratory furnace [15, 17] for the regulation of low pressure carburizing could be successfully be transposed to a real application. The main objective is to show qualitatively that the response of the probe could be used to determine the carbon flux and carbon potential at the surface of a given workload.

6.1 Contributions

The contributions of the research presented in this paper are the following:

- The results demonstrate that that a principle implemented in a laboratory furnace can indeed be applied in an industrial furnace.
- The results also show that the principle proved to be applicable within the context of atmospheric carburizing is still valid for low pressure conditions.
- The sample results indicate that this sensor indeed responds appropriately to a given carburizing atmosphere as it leads to the same conclusions than microhardness measurements and micrographical analysis.

Microhardness measurements and micrographical analysis are destructive methods and give information after the treatment while the sensor is a non-destructive one that provides information while the process is ongoing. This is the main advantage. To the best knowledge of the authors, the proposed probe is the only tool which is able to perform an *in-situ* carbon flux measurement during a low pressure carburizing treatment.

6.2 Future work

In further experiments, it will be interesting to test some other parameters (varying carburizing gas flow, mixture with neutral gas,...) in order to highlight a possible difference between acetylene, ethylene and propane. This is the subject matter of a project at ENSAM.

In the future, it is also planned to make some numerical predictions of the carbon diffusion across the probe's wall based on what is presented in section 2. Two-dimensional axisymmetric simulations are needed as the carbon content of the decarburizing gas and of the tube varies with the longitudinal axis of the tube. The resulting numerical model would enable the analyst to obtain the carbon profile and content within a part as a function of time. Moreover, there is a need for a better modeling of the variation of the diffusion coefficient with the carbide content. This should be investigated first in a one dimensional context.

Finally, numerical predictions could be validated with the use of another experimental technique such as WDS (Wave Dispersion Spectrometry).

7. REFERENCES

[1] Jacquet Ph., Bernard G.,Lambertin M. : Résultats expérimentaux liés au développement d'un capteur de suivi pour la cémentation basse pression. Traitements Thermiques n°323, pp73-75, 2000.

[2] Raic K. T., Numerical treatment of plasma carburizing process. Surface and Coatings Technology 92, pp. 22-28, 1997.

[3] Since J.J., « Infracarb » Process and Flexible Low Pressure Carburizing/Hardening Plants, 19th Heat Treating Society Conference, , Cincinnati, Ohio USA, 1-4 November 1999.

[4] Cyr G., La cémentation basse pression de micro – alésages Allcarb. Traitements Thermique n° 316, 1999.

[5] Sugiyama M., Ishikawa K., Iwata H., Vacuum Carburising with Acetylene, Advanced Materials and Processes, vol.4, pp.H29-H33, 1999.

[6] Hoffmann R., Cémentation sous vide : procédé i-Vacarb®, Traitement thermique n°295, pp22-23, 1996.

[7] Bond, H.W., Dispositif de mesure et de régulation du potentiel carbone: vue d'ensemble et historique. Traitement thermique, n°235, pp.29-31, 1990.

[8] Sobusiak, T., Method of mesuring carbon potential and carbon transfer coefficient. HEAT TREATMENT SHANGAI'83. Proceedings of the Third International Congress on Heat Treatment of Materials, Shangai, Edited by professor T. Bell, pp.1.79-1.85, 1983.

[9] Jacquet, P., Bernard, G., Jomain, B., Souchard, J.P., and Lambertin, M., Développement d'un capteur de suivi pour la cémentation basse pression des aciers, Traitement Thermique n°312, Novembre 1998.

[10] Jacquet, P., Cémentation basse pression des aciers. Développement d'un capteur de suivi, Thèse ENSAM, Cluny, 1998.

[11] Goldstein, J.I., and Moren, A. E., Diffusion modeling of the Carburization Process, Metallurgical transaction A, vol. 9A, pp. 1515-1525, 1978.

[12] Madsac, M., Queille, P., Kostelitz, M., Prévision des profils de concentration en carbone à partir d'un modèle de cémentation gazeuse, Application à l'optimisation des cycles thermiques. Traitement thermique, n°174, pp.19-25, 1983.

[13] Morral, J.E., Dupen, B.M., and Law, C.C., Application of Commercial Computer Codes to the Modeling Carburizing Kinetics of Alloy Steels. Metallurgical Transactions A, vol. 23A, pp. 2069-2071, 1992.

[14] Pavlossoglou, J., A new optimisation model of boost-diffusion cycle for infinite surface steel plates / cylinder to minimise time for desired carbon profile. HEAT TREATMENT SHANGAI'83. Proceedings of the Third International Congress on Heat Treatment of Materials, Shangai. Edited by professor T. Bell, pp.1.86-1.96, 1983.

[15] Stickels, C. A., Analytical Models for the Gas Carburizing Process. Metallurgical Transactions B, vol. 20B, pp. 535-546, 1989.

[16] Jacquet Ph., Bernard G.,Lambertin M. : Sensor tracks low-pressure carburizing, Advanced Materials and Processes, Heat Treating Progress, ppH19-H21, April 2000.

[17] Jacquet, P., Rousse, D., Bernard, G., Lambertin, M., Design of a novel device carburizing regulation, Metallurgy and New Materials Research, Vol.8, No.4, 2000.

[18] Ghiglione, D., Modèles mathématiques de cémentation, Traitement thermique, no195 , pp.31-39, 1985.

[19] Deshayes, J. Germain, P. Jacquot, E. Denisse, G. Dervieux, La cémentation basse pression des aciers. Traitement thermique, n°261 Janvier/ Février 1993, pp.22-30.

[20] Turdokan E.T., Martonik L.J., Kinetics of decarburization of austenite in hydrogen. High Temperature Science 2, pp154-168, 1970.

[21] Grabke H.J., Hörz G., Kinetics and mechanisms of gas-metal interactions, Ann. Rev. Mater. Sci., pp.155-178, 1977.

[22] Gräfen W., Edenhofer B., Acetylene low pressure carburizing. A novel and superior carburizing technology, Heat Treatment of Metals, pp. 79-83, 1999.

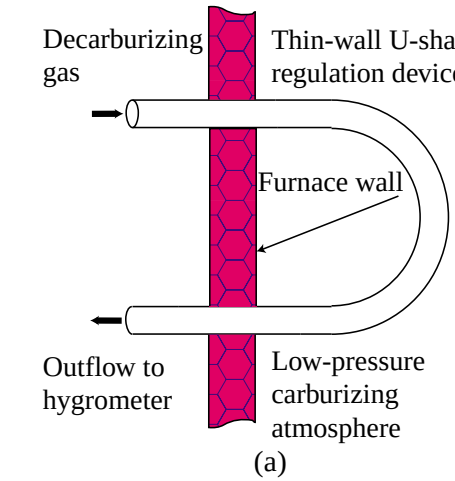

(a)

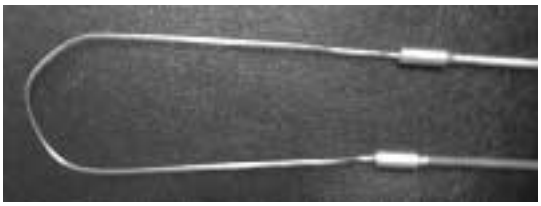

(b)

Figure 1: (a) Schematic of the U-shaped thin-wall device; (b) picture.

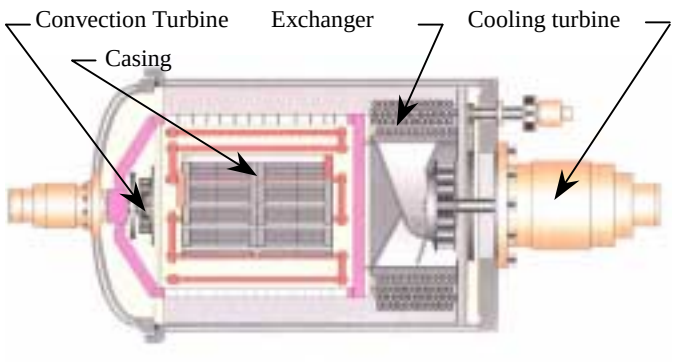

Figure 2: Schematic transversal view of the BMI B83 TiC furnace.

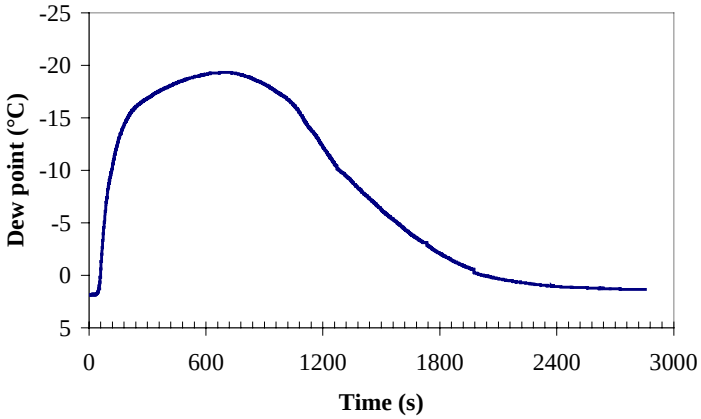

Figure 3 : Probe's response for a 90s carburizing + 40 min diffusion cycle.

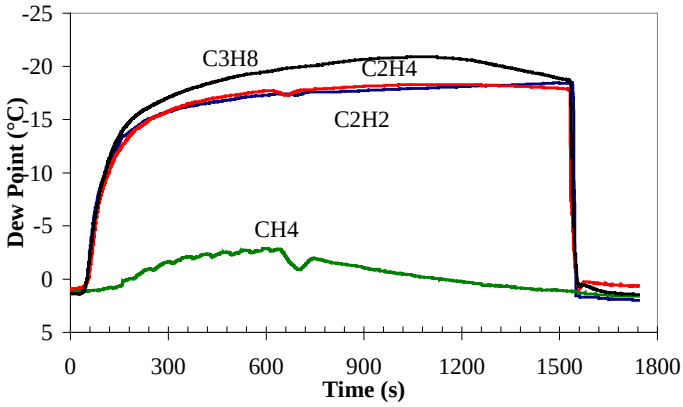

Figure 4 : Probe's responses for 4 different gases.

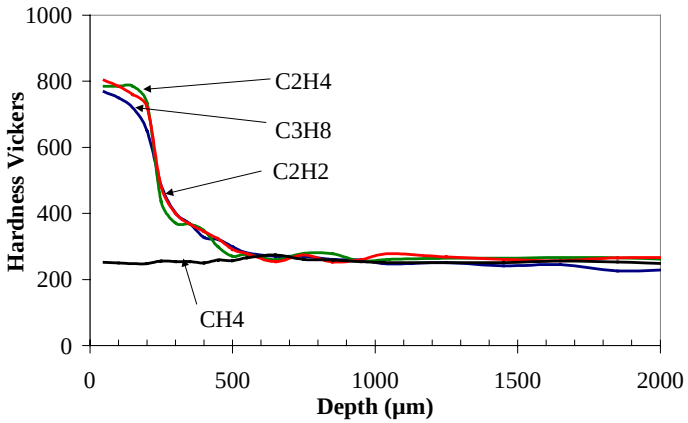

Figure 5 : Microhardness profiles after a standard low pressure carburizing treatment.

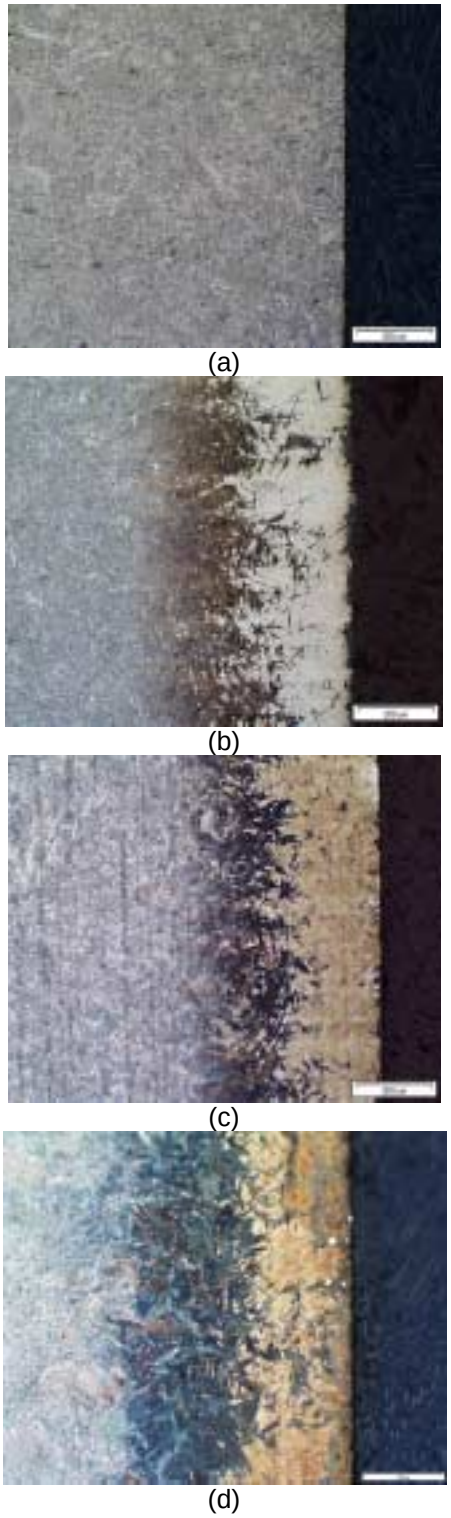

Figure 6 : MicrographiES after low pressure carburizing:
(a) methane; (b) acethylene; (c) ethylene; (d) propane.